

# Effects of Proton Irradiation on 60 GHz CMOS Transceiver Chip for Multi-Gbps Communication in High Energy Physics Experiments

---

I. Aziz,<sup>a,b,1</sup> D. Dancila,<sup>a</sup> S. Dittmeier,<sup>c</sup> A. Siligaris,<sup>d</sup> C. Dehos,<sup>d</sup> P. M. De Lurgio,<sup>e</sup> Z. Djurcic,<sup>e</sup> G. Drake,<sup>e</sup> J. L. G. Jimenez,<sup>d</sup> L. Gustaffson,<sup>a</sup> D. Kim,<sup>f</sup> E. Locci,<sup>g</sup> U. Pfeiffer,<sup>h</sup> P. Rodriguez Vazquez,<sup>h</sup> D. Röhrich,<sup>i</sup> A. Schoening,<sup>c</sup> H. K. Soltveit,<sup>c</sup> K. Ullaland,<sup>i</sup> P. Vincent,<sup>d</sup> S. Yang<sup>i</sup> and R. Brenner<sup>a</sup>

<sup>a</sup>*Uppsala University, Sweden*

<sup>b</sup>*Mirpur University of Science & Technology (MUST), Pakistan*

<sup>c</sup>*Heidelberg University, Germany*

<sup>d</sup>*CEA/LETI, France*

<sup>e</sup>*Argonne Laboratory, USA*

<sup>f</sup>*Gangneung-Wonju University, South Korea*

<sup>g</sup>*CEA/DSM/IRFU/DPhP & Paris-Saclay University, France*

<sup>h</sup>*Wuppertal University, Germany*

<sup>i</sup>*Bergen University, Norway*

*E-mail:* [imran.aziz@angstrom.uu.se](mailto:imran.aziz@angstrom.uu.se)

**ABSTRACT:** This paper presents the experimental results of 17 *MeV* proton irradiation on a 60 *GHz* low power, half duplex transceiver chip implemented in 65 *nm* CMOS technology. It supports short range point-to-point data rate up to 6 *Gbps* by employing on-off keying (OOK). To investigate the irradiation hardness for high energy physics applications, two TRX chips were irradiated with total ionizing doses (TID) of 74 *kGy* and 42 *kGy* and fluence of  $1.4 \times 10^{14}$  *Neq/cm*<sup>2</sup> and  $0.8 \times 10^{14}$  *Neq/cm*<sup>2</sup> for RX and TX modes respectively. The chips were characterized by pre- and post-irradiation analog voltage measurements on different circuit blocks as well as through the analysis of wireless transmission parameters like bit error rate (BER), eye diagram, jitter etc. Post-irradiation measurements have shown certain reduction in performance but both TRX chips have been found operational through over the air measurements at 5 *Gbps*. Moreover, very small shift in the carrier frequency was observed after the irradiation.

**KEYWORDS:** Radiation damage to electronic components, Radiation monitoring

ARXIV EPRINT: [1234.56789](https://arxiv.org/abs/1234.56789)

---

<sup>1</sup>Corresponding author.

---

## Contents

<b>1</b>	<b>Introduction</b>	<b>1</b>
<b>2</b>	<b>60 GHz CMOS Transceiver</b>	<b>2</b>
2.1	Transceiver Evaluation Board	2
<b>3</b>	<b>Proton Irradiation</b>	<b>4</b>
3.1	Irradiation Damages	4
3.2	Simulations and Calculations	4
<b>4</b>	<b>Irradiation Experiment</b>	<b>6</b>
4.1	Pre- and Post-Irradiation Results Comparison	8
<b>5</b>	<b>Conclusion and Future Work</b>	<b>10</b>

---

## 1 Introduction

The upgrade of accelerators and experiments at the Large Hadron Collider (LHC) for high luminosity will result in multiple times higher event rates, which demands high data rate readout systems [1]. For instance, the readout data requirement at the upgraded ATLAS silicon micro-strip tracker will be from 50 to 100 Tbps [2]. The transfer rate for highly granular tracking detectors is limited by the available bandwidth in current readout links [3]. Current readout systems typically use wired optical links which are immune to cross-talk but require large connectors size and are sensitive to mechanical damage.

Wireless data transmission using millimeter-wave technology has not yet been used in trackers for particle physics experiments. The Wireless Allowing Data and Power Transmission (WADAPT) collaboration [5] was formed to study the feasibility of wireless technologies in High Energy Physics (HEP) experiments. The objective is to provide a common platform for research and development in order to optimize the effectiveness and cost, with the aim of designing and testing wireless demonstrators for large instrumentation systems. A strong motivation for using wireless data transmission, is the absence of wires and connectors which will be an advantage in areas with low material budget. The availability of 9 GHz license-free bandwidth at 60 GHz (57-66 GHz) provides the opportunity to achieve multi-Gbps data rates for a single link. In addition, wireless transmission allows radial readout instead of current axial links, which opens for topological readout of tracking detectors. This can also reduce on-detector data volume using inter-layer communication, which will drastically reduce the readout time and latency [4].

Technology used in high energy physics (HEP) experiments, must withstand high radiation levels. The current detectors at LHC have accumulated radiation levels of approximately  $2 \times 10^{15} N_{eq}/cm^2$  and total ionizing dose (TID) of approximately 300 kGy. These values are expected

to increase tenfold for the high luminosity upgrade of LHC planned to be operational in 2026 [6]. With this target application in mind, we have performed an initial investigation into the radiation hardness of a low power, fully integrated 60 GHz wireless transceiver (TRX) chip. The TRX is fabricated in 65 nm CMOS technology targeting mobile devices requiring multi-Gbps data transfer. The chip was not designed for use in radiation environment, hence there were no guarantees for any functionality even after low doses. The irradiation was therefore done with a chip in operation to see in real time if the chip fails. The complexity of the setup limited the dose in this study, however, relevant results were obtained up to 74 kGy.

## 2 60 GHz CMOS Transceiver

The TRX chip under investigation has been manufactured by STMicroelectronics<sup>1</sup> in 65 nm CMOS technology. This V-band short-range chip can support point-to-point data rates from 10 Mbps to 6 Gbps by employing an on-off keying (OOK) modulation scheme. Moreover, it operates in half-duplex mode with power consumption of 40 mW in transmit mode, 25 mW in receive mode and 10  $\mu$ W in idle mode. The chip is packaged as a 25-ball very thin profile, fine-pitch ball grid array (VFBGA) with the overall dimensions of 2.2 mm x 2.2 mm x 1.0 mm. The low energy consumption as well as low profile of the chip make it a good candidate for the targeted applications. A modulation block diagram of the chip is shown in figure 1 (a). The carrier is generated in the transmitter subsystem by an on-chip voltage-controlled oscillator (VCO) which provides a differential sine-wave signal around 60.5 GHz. This signal is amplified to provide a large sine-wave to the modulator, while the amplification is controlled through feedback calibrated path. The amplified signal, along with the differential data from a line receiver, are fed to the OOK modulator. The output of the modulator is then transmitted through an antenna after amplification by the power amplifier (PA). In the receiver subsystem, the signal is passed through an on-chip low noise amplifier (LNA) and forwarded to non-coherent envelope detector. An adaptive comparator and baseband stages eliminate the duty cycle distortion and prove an error-free payload differential data stream at the output. The device maximizes flexibility by offering OFF, IDLE, RECEIVER and TRANSMITTER modes. The IDLE RX-sensing mode is optimized for very low power consumption and allows for automatic wake-up. In this mode, the receiver monitors and detects if any OOK modulation is present in order to wake-up the chip. Transition between different modes is achieved through direct configuration pins or through the I<sup>2</sup>C interface.

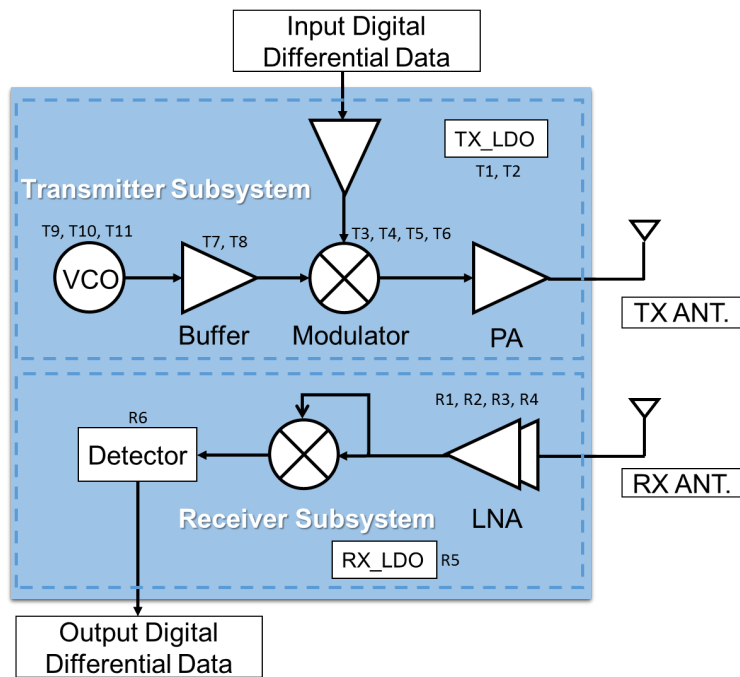
### 2.1 Transceiver Evaluation Board

Two test PCBs with TRX chips and required drive electronics have been prepared for chip characterization. As shown in figure 1 (b), the PCB has been provided with transmitter and receiver ports, as well as differential digital data ports. To monitor the power consumption of the chip separately, independent DC power ports have been made available for the chips and other drive electronics on the board. A DLN-4M adapter<sup>2</sup> has been used for I<sup>2</sup>C - USB interface. This allows the control and characterization of the chip through an embedded software via PC.

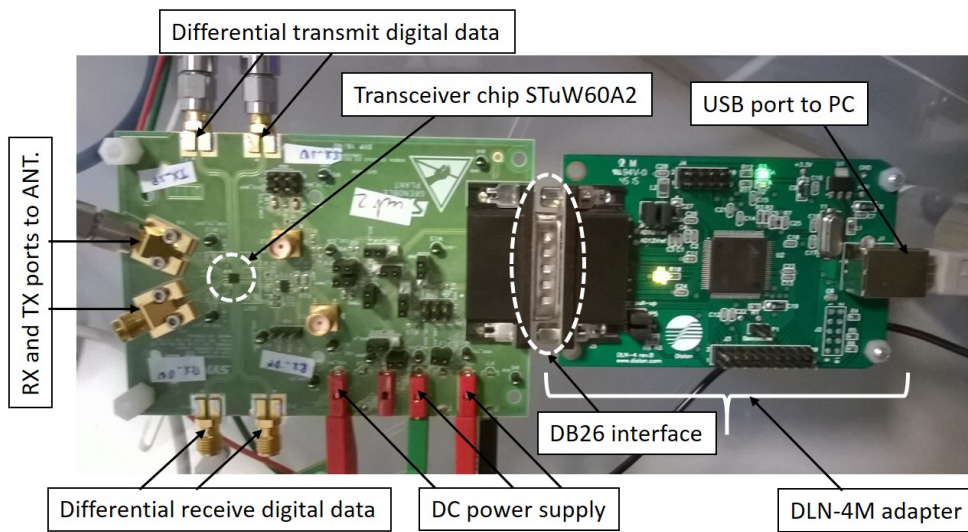
---

<sup>1</sup><https://www.st.com>

<sup>2</sup><https://diolan.com/dln-4m>



(a)



(b)

**Figure 1.** (a) Transceiver chip block diagram. T1 - T11 and R1 - R6 show analog voltage test points for transmitter and receiver subsystems, respectively. (b) Transceiver chip mounted on evaluation board, while DLN-4M adapter providing DB26 to USB interface

### 3 Proton Irradiation

The radiation damages in electronics for HEP experiment can be studied and approximated well with proton irradiation; even though protons will not be the most common particles in the HEP environment. The effects of proton irradiation can be scaled to and compared with the expected radiation environment in HEP experiments [7].

#### 3.1 Irradiation Damages

During irradiation, energy is deposited in semiconductors through electronic ionization and atomic collisions, resulting in ionization and displacement damages [8]. High ionizing radiation doses damage oxides and oxide/semiconductor interfaces [9]-[10], resulting in an increasing recombination current and degradation of the current gain [8]. In addition, atomic collision with semiconductor lattice creates vacancies and interstitial sites in crystal lattice, resulting in reduced carrier lifetime of semiconductor material, which in turn also degrades the current gain [11]. For silicon, the relation between proton energy and displacement damage ( $D(E)$ ), normalized to 1 MeV neutrons (95 MeVmb) is presented in figure 2. The curve shows that the protons being used in our study (17 MeV) are  $\sim 3.6$  times more damaging than 1 MeV neutrons.

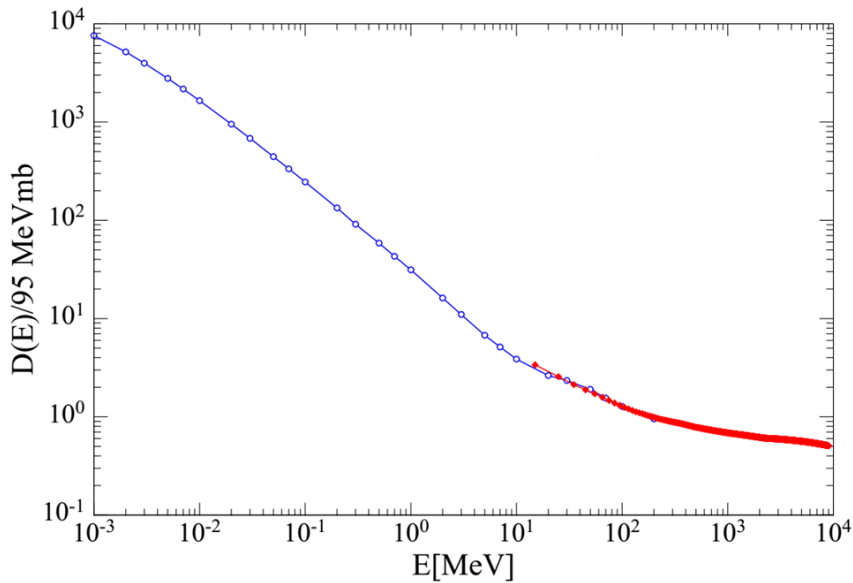


Figure 2. Proton induced displacement damage in Silicon [12] - [13]

#### 3.2 Simulations and Calculations

The software package FLUKA <sup>3</sup> has been used for simulations of particle transport and interactions with matter. As shown in the simulation setup in figure 3 (a), a proton beam is extracted from the cyclotron through a Havarfoil <sup>4</sup> window. A collimator is used to restrict the beam to an area

<sup>3</sup><http://www.fluka.org>

<sup>4</sup><http://www.goodfellow.com/E/Havar-High-Strength-Non-Magnetic-Alloy-Foil.html>

of  $3 \times 3 \text{ mm}^2$  to protect the surrounding electronics on the PCB. Both collimator and beam stop are made of lead (Pb). Given the unknown radiation hardness of the TRX chip, an initial fluence ( $F$ ) of about  $10^{14} N_{eq}/\text{cm}^2$  was selected. Figure 3 (b) shows the total ionizing dose (TID) per incident proton while neutron distribution is shown in figure 3 (c). These neutrons are secondary particles that could potentially damage electronics surrounding the TRX chip. It is further shown in figure 4 that a significant amount of energy is lost by the protons after passing through the TRX chip, indicating significant energy transfer to the DUT.

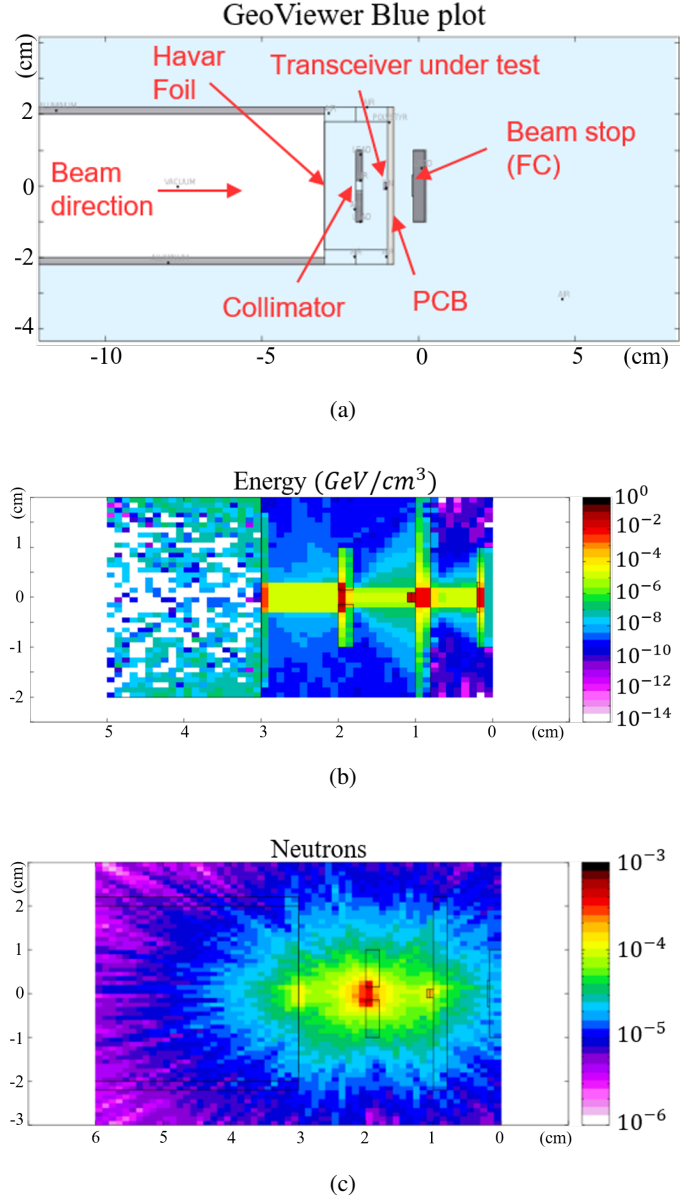


**Figure 3.** (a) Simulation setup (b) Total ionizing dose (TID) per incoming proton (c) Neutron yield per incoming proton

The simulated energy deposited in the transceiver chip,  $E_{sim}$  is  $28 \text{ MeV} / \text{cm}^3$  per incoming

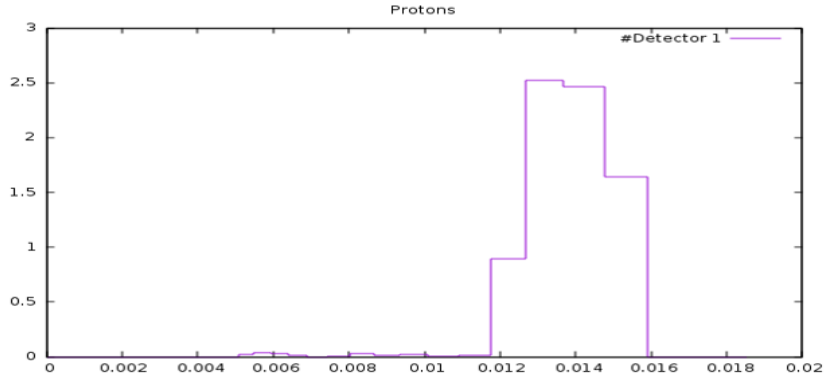


**Figure 4.** Simulated proton spectrum in irradiated silicon transceiver chip. The x-axis labels proton energy in GeV and the y-axis shows arbitrary units giving the relative amount of protons with a certain energy

proton, resulting in 192 kGy TID. To calculate the required time to achieve the target fluence ( $F$ ) of  $10^{14} N_{eq}/cm^2$ , we assume 1 nA beam current, which gives  $6.25 \times 10^9$  protons / s. As the collimator has restricted the irradiation area to  $3 \times 3 \text{ mm}^2$  ( $\sim 0.1 \text{ cm}^2$ ), with planned beam current, the required fluence from the accelerator can be achieved in

$$T_{irad} = F * A_{irad} / (S.F. * N_p) = 444 \text{ sec (7.4 min)} \quad (3.1)$$

where

$F$  = Target fluence ( $10^{14} N_{eq}/cm^2$ )

$A_{irad}$  = Effective irradiation area ( $0.1 \text{ cm}^2$ )

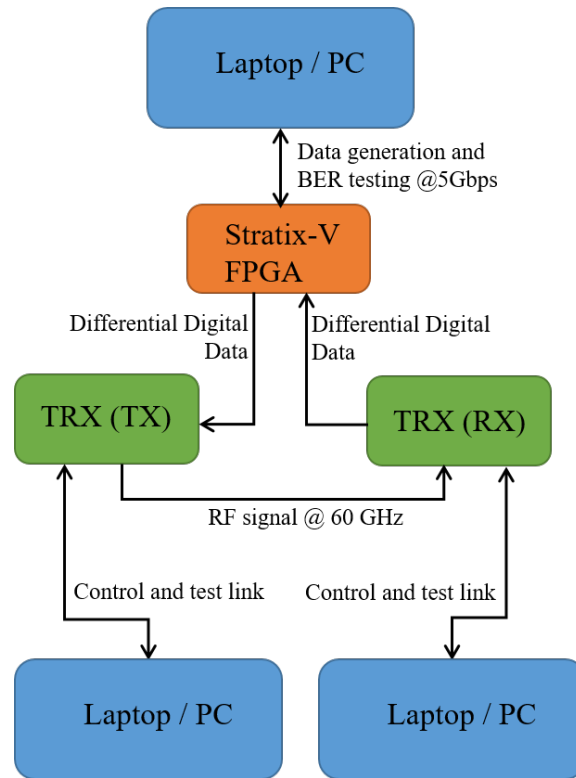
$S.F.$  = Damage Scaling Factor (3.6)

and  $N_p$  = No. of protons per second for 1 nA beam current ( $6.25 \times 10^9$ )

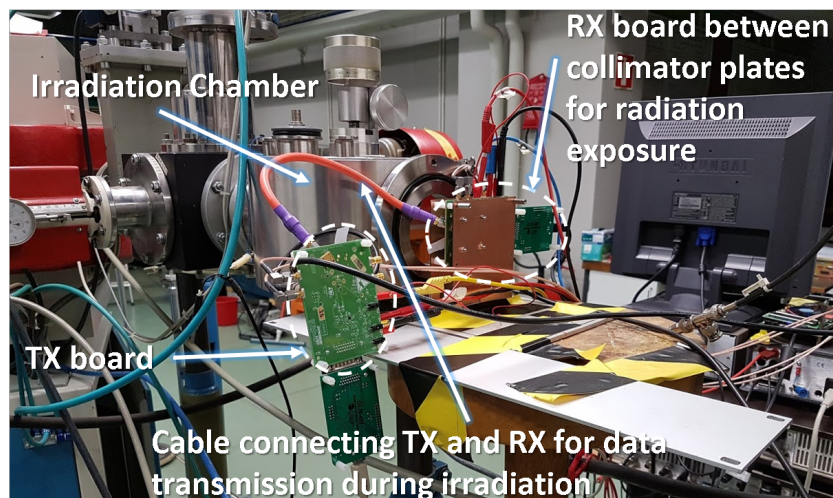
#### 4 Irradiation Experiment

The irradiation experiment was performed at Åbo Akademi University, Turku, Finland. Figure 5 (a) shows the block diagram of the measurement setup in the lab. A Stratix V FPGA board was used to generate a pseudo-random binary sequence 7 (PRBS7) at 5 Gbps. This data was sent as a differential pair to the transmitter TRX (TX), which further transmitted the 60 GHz modulated signal towards the receiver TRX (RX) module. To simplify the experimental setup, a coaxial cable connection was used between the the output of the TX board and the input of the RX board, as opposed to an over-the-air link with antennas. The RX forwarded the detected signal in differential pair to the Stratix V FPGA for data testing. The cyclotron (MGC-20) was set to 17 MeV protons and the TRX evaluation board operating in RX mode was placed on the beam line attached to the irradiation chamber with an air propagation distance of 30 cm between the beam aperture and the chip. As shown in figure 5 (b), the board is fitted between the collimator plates and both boards are connected by the coaxial cable, during the irradiation.

Additionally, the film dosimeter was placed on top of the TRX to record the cumulative dose. The RX chip was irradiated first, as it requires a pristine TX chip to test, while the chip can be evaluated in TX mode in isolation, without the RX. Each irradiation experiment was done in three



(a)



(b)

**Figure 5.** (a) Block diagram of measurement setup at cyclotron facility, RX and TX were in turn exposed to high energy beam (b) Irradiation experimental setup at Åbo Akademi University, Finland

steps with increasing beam current. Before the irradiation, a calibration experiment was performed with only the irradiation setup (collimator and beam stop) to determine the beam current. These beam current calibrations were used for the fluence and dose calculations given in table 1. The values

are lower for the TX because the TRXs were characterized multiple times during the irradiation, which made the cyclotron filament move out of apex towards the end of the experiment when the TX was being exposed.

**Table 1.** Calculated fluences and doses during irradiation

DUT	Calculated Fluence ( $N_{eq}/cm^2$ )	Calculated TID ( $kGy$ )
RX	$1.38 \times 10^{14}$	74
TX	$0.78 \times 10^{14}$	42

#### 4.1 Pre- and Post-Irradiation Results Comparison

After the experiment, both TRX PCBs were stored in a freezer for 3 weeks to minimize the annealing while waiting for the activity to decay. In the post-irradiation analysis, both the RX and the TX have been found functional through over-the-air measurements at 5 Gbps. The comparison of pre- and post-irradiation analog voltage measurements for the test points shown in figure 1(a), is tabulated in table 2. For the TX, low dropout voltages (T1 & T2), mixer voltages (T3 & T4), modulator voltages (T5 & T6), buffer voltages (T7 & T8) and VCO voltages (T9, T10 & T11) are presented. For the power management (PM), bandgap voltage (VBG) is measured and for the RX, two stage LNA voltages (R1, R2, R3 & R4), baseband LDO voltage (R5), gate bias detector voltage (R6) and amplitude control signal voltage (VATC) are tabulated. It can be observed that there is no significant difference in the pre- and post-irradiation measurements for the TX, but that the RX chip looks comparatively more affected by the irradiation. This is in accordance with the provided TID and fluence. Likewise, a power consumption comparison is presented in table 3. The measurements were taken for an active transmission link (Data-ON) and without data (Data-OFF). These results also show notable differences in pre- and post- irradiation measurements for the RX compared to the TX. Further analysis revealed a reduction in the TX power and the RX gain by 1 dB and 4.5 dB, respectively. Sufficient link budgeting can fully compensate the reduction in the TX power, while up to 2 dB loss in the RX gain can also be recovered. In addition, the RX envelope detector and digital interface remained unaffected by the irradiation. Moreover, a spectrum analyzer <sup>5</sup> with external V-band mixer was used in the pre-, post- and during-irradiation characterizations to monitor the RF power level as a function of frequency. The normalized power spectrum of 5 Gbps data transmission is shown in figure 6. The transmitter was set on continuous wave mode and a small downshift of 10 MHz in the center frequency was observed after the irradiation. This is in agreement with the results from RD-53 collaboration [14] at CERN. From their studies we can expect higher doses to shift the central frequency even more. However, as the chip uses the envelope detection in RX mode, this shift will not affect the communication.

The test setup for wireless data measurement at 5 Gbps with the help of horn antennas is shown in figure 7 (a). The corresponding eye diagram with the RMS jitter of 21 ps, 60 mV eye height and 67 ps eye width is presented in figure 7 (b). A similar level of jitter was obtained in post-irradiation

<sup>5</sup>Keysight Technologies 11970V 50-75 GHz Series Harmonic Mixer

**Table 2.** Pre- and post-irradiation analog test comparison at 5 Gbps

Transmitter (TX)			Receiver (RX)		
Test	Pre (V)	Post (V)	Test	Pre (V)	Post (V)
LDO1 (T1)	1.006	1.007	VDDA (R1)	1.116	1.079
LDO2 (T2)	1.207	1.208	VGGA (R2)	0.558	0.497
VDDA (T3)	1.007	1.008	VDDA (R3)	1.115	1.077
VGGA (T4)	0.710	0.706	VGGA (R4)	0.555	0.491
VDDA (T5)	0.990	0.992	LDO-BB (R5)	1.219	1.177
VGGA (T6)	0.517	0.517	VGDET (R6)	0.215	0.216
VDDA (T7)	0.993	0.995	VATC	0.972	0.940
VGGA (T8)	0.509	0.509	-	-	-
VDDA (T9)	0.516	0.563	-	-	-
VGGA (T10)	0.633	0.636	-	-	-
Vtune (T11)	0.669	0.661	-	-	-
VBG (PM)	1.206	1.207	-	-	-

**Table 3.** Pre- and post-irradiation power consumption for TX and RX

Test Name	Pre-irradiation consumption	Post-irradiation consumption
TX-Data-OFF	33.9 mW	32.4 mW
TX-Data-ON	40.6 mW	43 mW
RX-Data-OFF	15.2 mW	11.4 mW
RX-Data-ON	14.7 mW	7.8 mW

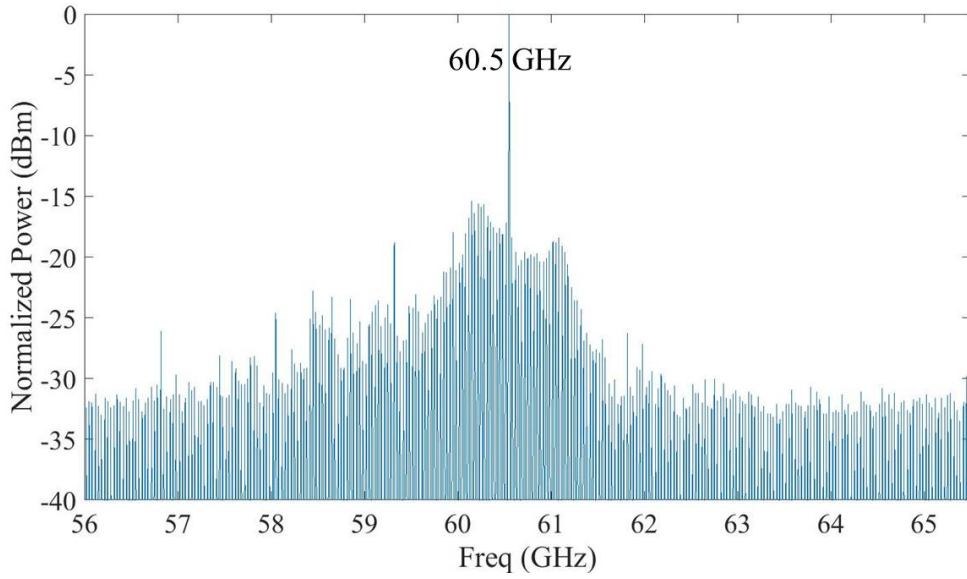


**Figure 6.** Normalized power spectrum of 5 Gbps data transmission while transmitter was set on continuous wave mode. Highest peak is at 60.5 GHz

**Table 4.** Pre- & post-irradiation wireless BER test for  $10^{12}$  tested bits

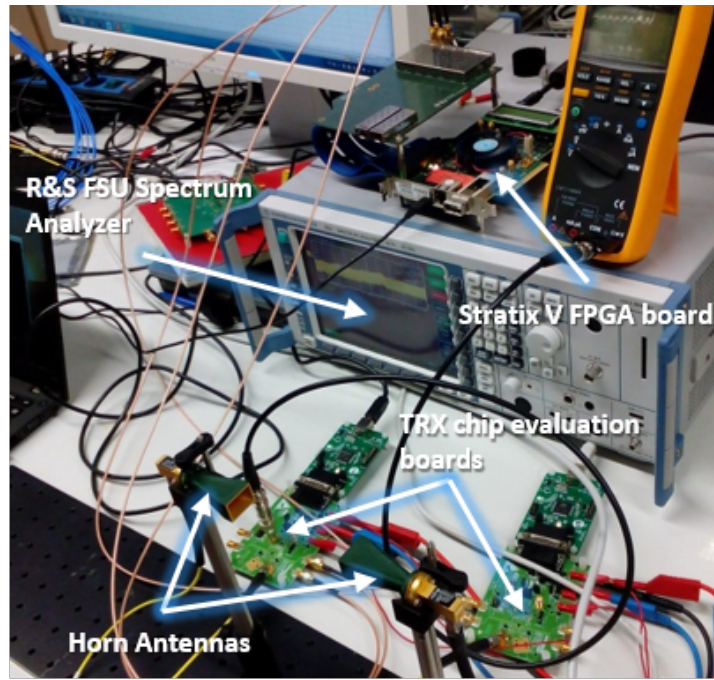
Distance (cm)	Pre-irradiation BER	Post-irradiation BER
6	0	0
8	0	$1.4 \times 10^{-10}$
10	0	$9.0 \times 10^{-6}$

measurements with comparatively reduced range. Similar findings are presented in table 4 as pre- and post-irradiation BER test results at 1.25 Gbps for  $10^{12}$  tested bits.

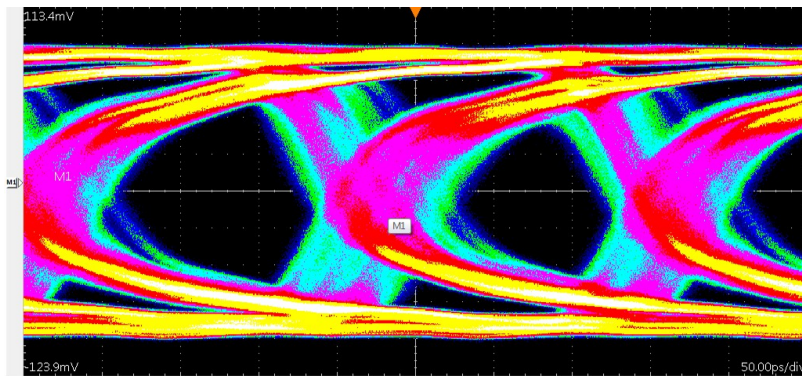
## 5 Conclusion and Future Work

The radiation hardness of a V-band TRX chip in 65nm CMOS, acting both in TX and RX modes was investigated after 17 MeV proton irradiation. TID and fluence used during the experiment were 74 kGy & 42 kGy and  $1.4 \times 10^{14} N_{eq}/cm^2$  &  $0.8 \times 10^{14} N_{eq}/cm^2$  for the RX & the TX, respectively. The RX experienced higher loss of sensitivity than the TX power loss, which is in accordance with the respective TID and fluence. However, both the RX and the TX were found operational through over the air measurements at 5 Gbps after irradiation with losses that can be compensated through link budgeting.

The experiment shows that the chip may be used successfully in a radiation environment, despite the fact that the devices were not specifically radiation hardened by either design or by



(a)



(b)

**Figure 7.** 5 Gbps wireless measurements (a) Point-to-point wireless link established with horn antennas (b) Eye diagram from Tektronix DSA8300 Digital Serial Analyzer

process. In future, these TRX ICs will be tested at higher doses to analyze the technological limitations.

### Acknowledgment

The authors would like to thank Pierre Busson, Nicolas Ricome and Frederic Lagrange from STMicroelectronics for providing equipment and support as well as Åbo Akademi University, Finland for use of their irradiation facility. Imran Aziz is thankful to MUST, Pakistan for their financial assistance and Sebastian Dittmeier acknowledges support by the International Max Planck Research School for Precision Tests of Fundamental Symmetries.

## References

- [1] S. Dittmeier, N. Berger, A. Schöning, H.K. Soltveit, and D. Wiedner. 60 GHz wireless data transfer for tracker readout systems - First studies and results. *Journal of Instrumentation*, 9(11), 2014.
- [2] R Brenner and S Cheng. Multigigabit wireless transfer of trigger data through millimetre wave technology. *Journal of Instrumentation*, 5(07):c07002–c07002, 2010.
- [3] H K Soltveit, R Brenner, and D Wiedner. Multi-Gigabit Wireless data transfer at 60 GHz. 12016, 2012.
- [4] S. Dittmeier, R. Brenner, D. Dancila, C. Dehos, P. De Lurgio, Z. Djurcic, G. Drake, J.L. Gonzalez Gimenez, L. Gustafsson, D.-W. Kim, E. Locci, U. Pfeiffer, D. Röhrich, A. Rydberg, A. Schöning, A. Siligaris, H.K. Soltveit, K. Ullaland, P. Vincent, P. Rodriguez Vazquez, D. Wiedner, and S. Yang. Wireless data transmission for high energy physics applications. *EPJ Web of Conferences*, 150:1–8, 2017.
- [5] R. Brenner, S. Ceuterickx, C. Dehos, P. De Lurgio, Z. Djurcic, G. Drake, J. L. Gonzalez Gimenez, L. Gustafsson, D. W. Kim, E. Locci, D. Roehrich, A. Schoening, A. Siligaris, H. K. Soltveit, K. Ullaland, P. Vincent, D. Wiednert, and S. Yang. Development of Wireless Techniques in Data and Power Transmission - Application for Particle Physics Detectors. pages 1–20, 2015.
- [6] Michael Moll. Displacement Damage in Silicon Detectors for High Energy Physics. *IEEE Transactions on Nuclear Science*, 65(1):1–1, 2018.
- [7] S. Díez, M. Lozano, G. Pellegrini, F. Campabadal, I. Mandić, D. Knoll, B. Heinemann, and M. Ullán. Proton radiation damage on SiGe: C HBTs and additivity of ionization and displacement effects. *IEEE Transactions on Nuclear Science*, 56(4):1931–1936, 2009.
- [8] Jianqun Yang, Xingji Li, Chaoming Liu, and Daniel M. Fleetwood. The effect of ionization and displacement damage on minority carrier lifetime. *Microelectronics Reliability*, 82(January):124–129, 2018.
- [9] T. P. Ma and Paul V. Dressendorfer. *Ionizing Radiation Effects in MOS Devices and Circuits*. 1989.
- [10] J.P. Raymond and E.L. Petersen. Comparison of Neutron, Proton and Gamma Ray Effects in Semiconductor Devices. *IEEE Transactions on Nuclear Science*,, Vol. NS-34(December 1987):37–41, 1987.
- [11] E. Minson, I. Sanchez, H. J. Barnaby, R. L. Pease, D. G. Platteter, and G. Dunnam. Assessment of gated sweep technique for total dose and dose rate analysis in bipolar oxides. *IEEE Transactions on Nuclear Science*, 51(6 II):3723–3729, 2004.
- [12] Geoffrey P. Summers, Edward A. Burke, Philip Shapiro, Scott R. Messenger, and Robert J. Walters. Damage correlations in semiconductors exposed to gamma, electron and proton radiations. *IEEE Transactions on Nuclear Science*, 40(6):1372–1379, 1993.
- [13] M Huhtinen and P A Aarnio. Letter to the Editor Pion induced displacement damage in silicon devices. *Nuclear Physics B*, 335:580–582, 1993.
- [14] <https://rd53.web.cern.ch/RD53/>.